Development 136, 2413-2422 (2009) doi:10.1242/dev.029165

The RNA-binding protein Mex3b has a fine-tuning system for mRNA regulation in early *Xenopus* development

Hitomi Takada[1,2], Takahiro Kawana[1], Yuzuru Ito[3], Reiko F. Kikuno[4], Hiroshi Mamada[1], Toshiyuki Araki[2], Hisashi Koga[4], Makoto Asashima[3,5] and Masanori Taira[1,*]

Post-transcriptional control by RNA-binding proteins is a precise way to assure appropriate levels of gene expression. Here, we identify a novel mRNA regulatory system involving Mex3b (RKHD3) and demonstrate its role in FGF signaling. *mex3b* mRNA has a 3′ long conserved UTR, named 3′LCU, which contains multiple elements for both mRNA destabilization and translational enhancement. Notably, Mex3b promotes destabilization of its own mRNA by binding to the 3′LCU, thereby forming a negative autoregulatory loop. The combination of positive regulation and negative autoregulation constitutes a fine-tuning system for post-transcriptional control. In early embryogenesis, Mex3b is involved in anteroposterior patterning of the neural plate. Consistent with this, Mex3b can attenuate FGF signaling and destabilize mRNAs for the FGF signaling components Syndecan 2 and Ets1b through their 3′ UTRs. These data suggest that the 3′LCU-mediated fine-tuning system determines the appropriate level of *mex3b* expression, which in turn contributes to neural patterning through regulating FGF signaling.

KEY WORDS: FGF, Mex3b, RNA-binding protein, *Xenopus*, Neural plate, Post-transcriptional regulation

INTRODUCTION

In developmental processes, embryonic induction and patterning are strictly regulated in a spatiotemporal manner by the expression of numerous genes. Gene expression can be regulated at multiple steps, including transcription, mRNA stability and translation. For gene expression to be established at an appropriate level, some of these regulatory processes must be under rapid and precise control. Because transcriptional regulation is not sufficient to determine the level of gene expression and its duration, post-transcriptional regulation is necessary for fine-tuning gene expression. Fine-tuning mechanisms, such as the regulation of mRNA stability and translational efficacy, are generally operated by cis-elements present mostly in 3′ untranslated regions (UTRs) and by trans-acting factors, such as RNA-binding proteins and miRNA (Kuersten and Goodwin, 2003; Sevignani et al., 2006). These regulators can adjust the amounts of gene products and the duration of gene expression more rapidly and precisely than can transcriptional regulation. With respect to signal transduction, maintaining certain levels of signal transduction components such as ligands, receptors, co-receptors, cytoplasmic transducers and transcription factors is thought to be crucial for transducing appropriate levels of signaling. Thus, although post-transcriptional regulation needs to be incorporated into the control mechanisms for determining the levels of signal transduction components, its mechanisms remain poorly understood.

[1]Department of Biological Sciences, Graduate School of Science, University of Tokyo, 7-3-1 Hongo, Bunkyo-ku, Tokyo 113-0033, Japan. [2]Department of PNS research, National Institute of Neuroscience, National Center of Neurology and Psychiatry (NCNP), 4-1-1 Ogawahigashi, Kodaira, Tokyo 187-8502, Japan. [3]Organ Development Research Laboratory, National Institute of Advanced Industrial Sciences and Technology (AIST), Tsukuba Central 4, 1-1-1 Higashi, Tsukuba, Ibaraki 305-8562, Japan. [4]Department of Human Genome Research, Kazusa DNA Research Institute, 2-6-7 Kazusa-Kamatari, Kisarazu, Chiba 292-0818, Japan. [5]Department of Life Science, Graduate School of Arts and Sciences, The University of Tokyo, 3-8-1 Komaba, Meguro-ku, Tokyo 153-8902, Japan.

*Author for correspondence (e-mail: m_taira@biol.s.u-tokyo.ac.jp).

Accepted 28 April 2009

RNA-binding proteins have been shown to play key roles in post-transcriptional control. RNA-binding proteins are classified into several families according to the types of RNA-binding domains they contain: Zn finger proteins; RNA recognition motif (RRM) proteins, such as ELAV/Hu, Musashi-1/Nrp1 and SRp38; and KH (hnRNP K homology) domain proteins, such as Mex3. In vertebrate development, for example, ELAV family members are involved in neuronal differentiation by stabilizing target mRNAs (Perrone-Bizzozero and Bolognani, 2002). RNA-binding proteins are also involved in subcellular RNA localization in oocytes and asymmetrically dividing cells (Minakhina and Steward, 2005). Despite these studies, RNA-binding proteins have not been reported to be involved in functions of early vertebrate development such as anteroposterior (AP) patterning and signal transduction.

With respect to cis-elements in 3′ UTRs and trans-acting factors for the regulation of mRNA stability and translation, AU-rich elements (AREs), typically the AUUUA sequence, and their binding proteins have been well investigated. To date, many ARE-containing mRNAs, such as those for Fos and Myc, have been reported to be subject to rapid degradation by RNA-binding proteins, such as AUF1 and Tristetraprolin (TTP) (Barreau et al., 2005; Chen and Shyu, 1995). These mRNAs are all short-lived and are rapidly degraded when transcription is stopped. However, other types of destabilizing elements have not been fully investigated, especially in developmental processes.

In the course of seeking novel genes from a *Xenopus* anterior neuroectoderm cDNA library using expression pattern screening (Takahashi et al., 2005), we identified a gene encoding an RNA-binding protein, Mex3b, which possesses two KH domains and a RING finger domain. A notable feature of this gene is the possession of a long evolutionarily conserved region in the 3′ UTR, named 3′ long conserved untranslated region (3′LCU), which is 800 nucleotides long and is highly conserved among vertebrates. Mex-3 has been identified in *Caenorhabditis elegans*, ascidians and sea urchins, and a family of four paralogous proteins, MEX3A, MEX3B, MEX3C and MEX3D, has been identified in humans (Buchet-Poyau et al., 2007). *mex-3* mRNA is localized in the anterior blastomeres of *C. elegans* embryos, and its product, MEX-

3, determines anterior characteristics by repressing the expression of *pal-1*, which encodes a Caudal-like homeodomain protein (Draper et al., 1996; Huang et al., 2002). *pem-3*, an ascidian ortholog of *mex-3*, plays a role in the differentiation of the brain of ascidian larvae (Satou, 1999). However, the molecular mechanisms of MEX-3 and PEM-3 functions remain to be elucidated. In humans, MEX3D (also known as TINO or RKHD1) has been shown to destabilize *BCL2* mRNA by binding to its ARE (Donnini et al., 2004), and MEX3C (also known as RKHD2) is putatively involved in the congenital human disease 'essential hypertension' (Guzman et al., 2006). However, the developmental role of *mex3* genes in vertebrate embryos has not yet been investigated, and the existence of the 3′LCU has not been reported.

In this study, we investigated the function of *mex3b* in early *Xenopus* embryogenesis and the role of the 3′LCU in mRNA regulation. We found that the 3′LCU controls the level of *mex3b* expression through the regulation of both translational enhancement and autoregulatory destabilization of the mRNA. Functional analyses suggest that Mex3b is required for AP patterning and mesoderm formation, and that Mex3b attenuates FGF responsiveness by destabilizing the FGF signaling components Syndecan 2 (Sdc2) and Ets1 through their 3′ UTRs.

MATERIALS AND METHODS

Embryo manipulations, β-gal staining and whole-mount in situ hybridization

Artificial fertilization, rearing of embryos and animal cap assays were performed as described previously (Shinga et al., 2001; Taira et al., 1992). FGF2/bFGF or activin were used. Embryonic stages were determined according to Nieuwkoop and Faber (Nieuwkoop and Faber, 1967). β-Gal staining and whole-mount in situ hybridization (WISH) was carried out as described previously (Suga et al., 2006; Takada et al., 2005).

Plasmid construction and in vitro mRNA synthesis

The full-length clone of *Xenopus mex3b* (DDBJ accession no. AB499902) was obtained from Open Biosystems. The following plasmids were constructed for functional analysis. The *mex3b* coding sequence (CDS) was PCR-amplified and cloned into the *Cla*I and *Eco*RI sites of pCS2+ to construct pCS2+Mex3b. N-terminally Myc-tagged Mex3b constructs, pCS2+Myc-Mex3b and pCS2+Myc-ΔKH1+2, were made by inserting PCR products of the *mex3b* and ΔKH1+2 (aa 58-124 and 157-220 were deleted) CDSs into the *Eco*RI and *Xba*I sites of pCS2+MTmcs (made by H.T. and M.T.). C-terminally HA-tagged Mex3b constructs, pCS2+Mex3b-HA and pCS2+ΔKH1+2-HA, were made by inserting PCR products of the coding region of Mex3b and ΔKH1+2 CDSs into the *Cla*I site of pCS2+mcs4HAmcs (made by S. Matsuda and M.T.). To construct pCS2+*myc-mex3b*-3′LCU and pCS2+*mex3b-HA*-D for DNA expression, PCR products of the 3′LCU and subregion D were inserted into the *Xba*I site of pCS2+Myc-Mex3b and the *Eco*RI site of pCS2+Mex3b-HA, respectively. The following constructs were used for GFP mRNA reporter experiments. The 3′LCU (nucleotide nos 1-798), BCD (nos 244-798), CD (nos 405-798), D (nos 577-798), ABC (nos 1-576), AB (nos 1-404), and A (nos 1-243) were PCR-amplified with the N25A3 clone (DDBJ accession no. AB499903) and inserted into the *Xba*I site downstream of the GFP CDS of pCS2+AdN-GFP (made by M. Inamori and M. T.). To construct a destabilized GFP reporter plasmid, pCS105-GFP-PEST, the region encoding the PEST sequence of ornithine decarboxylase was PCR-amplified from a stage 17/18 *Xenopus* cDNA library and inserted into the *Eco*RI and *Xba*I sites downstream of the GFP CDS in pCS105+GFPn (made by S. Osada and M. T.). To construct pCS105-GFP-PEST+3′LCU, +3′LCUrev, and +nc3′UTR, the corresponding regions were PCR-amplified and inserted into the *Xba*I site of pCS2+GFP-PEST. To construct pCS2+GFP+fgf20-3′UTR, +sdc2-3′UTR, +ets1b-3′UTR, and +syntenin-3′UTR, those 3′ UTR sequences were PCR-amplified from a stage 17/18 *Xenopus* cDNA library, and inserted into the *Xba*I site of pCS2+AdN-GFP.

Microarray analysis

The microarray tips that we used have 40,000 spots, each of which contained a 60mer oligonucleotide designed based on unique sequences near the 3′ ends of known or unknown cDNA or expressed sequence tag (EST) clones deposited in GenBank/DDBJ as Unigene. Total RNA was extracted from dissected neural plate tissue and reverse-transcribed with the oligo(dT) primer containing the T7 promoter. Cy3- or Cy5-labeled cRNA was synthesized from a cDNA pool and purified with RNeasy (Qiagen). Cy-labeled cRNA was then fragmented and hybridized to microarray glasses (Agilent Technology) at 65°C overnight.

Western blot analysis

Injected embryos were homogenized with cell lysis buffer (20 mM Tris-HCl, pH 8.0, 1 mM EDTA, 8 mM DTT, 40 μg/ml leupeptin, 20 μg/ml aprotinin, 2 mM PMSF, 0.1% NP-40). Protein bands on a polyvinylidene fluoride (PVDF) membrane were visualized using anti-Myc (9E10; BIOMOL) and anti-HA (Y-11; Santa Cruz) antibody as primary antibody and Alexa Fluor 680 anti-mouse IgG antibody (Molecular Probes) as secondary antibody, or using anti-GFP antibody conjugated with Irdye800 (ROCKLAND), and quantified with the Odyssey System (Aloka).

RNA immunoprecipitation

RNA immunoprecipitation experiments were performed as described previously (Liu and Harland, 2005). Embryos were lysed at stage 8.5 with homogenize buffer (15 mM HEPES, pH 7.6, 10 mM KCl, 1.5 mM $MgCl_2$, 0.5 mM EGTA, 44 mM sucrose, 8 mM DTT, 40 μg/ml leupeptin, 20 μg/ml aprotinin, 2 mM PMSF, 40 units/ml RNasin). Supernatants were incubated with anti-HA antibody (prepared from ascites of 9E10 cell-inoculated mice by Y. Goya, Y. Mii, M. Park and M.T.) for 1 hour, and then incubated with protein G agarose beads for another hour. The beads were washed three times with homogenize buffer, and treated with proteinase K in lysis buffer (0.5% SDS, 5 mM EDTA, 50 mM Tris-HCl, pH 7.5, 50 mM NaCl) for 45 minutes. The resultant solution with the beads was treated with phenol/chloroform, and nucleic acids were isolated for RT-PCR with a GFP primer set (forwards: 5′-AACGGCCACAAGTTCAGCGTGTCCG-3′; reverse: 5′-CAGGACCATGTGATCGCGCTTCTCG-3′).

Antisense morpholino oligo experiments

Two antisense morpholino oligos designed for 25-nucleotide sequences upstream of the start codon of *mex3b* (Mex3bMO1, 5′-GCTCACCTCAGTGCTACGTACAGAC-3′; and Mex3bMO2, 5′-TTCCTTCCGTTACCCCTGAGTATTG-3′), and a five-base mismatched control oligo for Mex3bMO1 (5mmMO, 5′-GFTgACCTgAG-TcCTACcTACAcAC-3′) were purchased from Gene Tools.

Luciferase reporter assay

Embryos were co-injected with *cdx4/Xcad3-luc*, which contains the –546 promoter sequence and the entire intron 1 region of *cdx4*, or TOPFLASH DNA reporter (Haremaki et al., 2003; van de Wetering et al., 1997) together with mRNA or DNA expression plasmid into the two ventral animal blastomeres at the four-cell stage. Five pools of three injected embryos or animal caps were assayed for luciferase activity at stage 12.5/13 using the luciferase assay system (Promega) according to the manufacturer's protocol, as described (Yamamoto et al., 2003).

Real-time PCR

Real-time PCR analysis for quantitative RT-PCR (qRT-PCR) was performed using ABI PRISM 7000 or 7300 detection systems with Power SYBR Green PCR Master Mix and PCR primers as follows: reporter mRNA (designed for the SV40 polyadenylation region in the 3′ UTR): forward, 5′-TCGTATTACGTAGATCCAGACA-3′; reverse, 5′-TGGTTACAAA-TAAAGCAATAGCATC-3′; *ef1α*: forward, 5′-CCCTGCTGGAAG-CTCTTGAC-3′, reverse, 5′-GAGGCAGACGGAGAGGCTTAT-3′; SV40: *gapdh*: forward, 5′-AGTTGGCGTGAACCATGAGA-3′, reverse, 5′-CGTTGATGACCTTTGCGAGA-3′. All real-time PCR assay was performed in triplicate. Values of reporter mRNA were quantitated using an appropriate standard curve, and were normalized with those of the internal control, *ef1α* or *gapdh*. Error bars of normalized values were calculated using a standard technique from deviations of three values.

RESULTS

Characterization and expression of *Xenopus mex3b*

Our previous expression-pattern screening of an anterior neuroectoderm cDNA library (Takahashi et al., 2005) identified a clone, N25A3, which has a 0.8 kb conserved noncoding sequence. EST analysis of N25A3 and sequencing of its full-length cDNA clone revealed that the N25A3 sequence is a part of the 3′ UTR of an mRNA with a CDS that encodes 507 amino acids containing two KH domains and a RING finger domain. This gene was subsequently identified as the *Xenopus* ortholog of human MEX3B (also known as RKHD3) (Fig. 1A). The 3′ UTR of *Xenopus mex3b* is 2.2 kb long and, notably, the last 0.8 kb sequence is highly conserved among vertebrates and amphioxus (see Fig. S1 in the supplementary material). This sequence will be referred to as '3′ long conserved UTR' (3′LCU) (Fig. 1B,C). Database analysis suggests that such a long evolutionarily conserved 3′ UTR is very unusual, implying that the 3′LCU plays an important and unique role in the regulation of *mex3b* mRNA. Because KH domains are believed to be an RNA-binding domain, we hypothesized that Mex3b protein regulates its target RNAs through KH domains and that the 3′LCU of *mex3b* mRNA is involved in post-transcriptional regulation by RNA-binding proteins.

In *Xenopus* embryos, *mex3b* mRNA was detected in the animal region at the four-cell stage (Fig. 1D,E). At the early gastrula stages, *mex3b* was expressed in the entire ectoderm and the equatorial region (Fig. 1F,G). During gastrulation, the expression in the ectoderm region gradually became restricted to the neural plate during gastrulation (Fig. 1H,I). At later stages, expression was detected in the brain, branchial arches and tailbud (Fig. 1J). This expression pattern implies multiple functional roles of *mex3b* in embryogenesis.

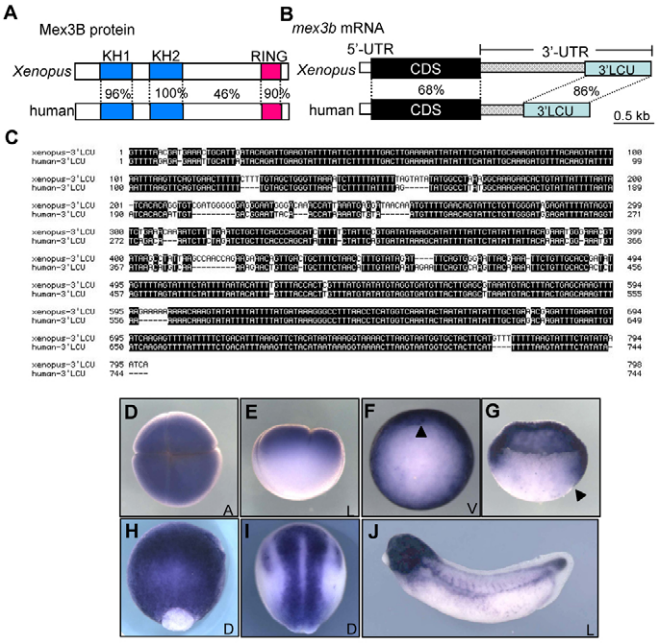

Fig. 1. Characterization of *mex3b*. (**A**,**B**) Schematic representations of *Xenopus* and human Mex3b/MEX3B proteins (A) and *mex3b*/*MEX3B* mRNAs (B). Sequence identities are indicated. Note that the identity of the 3′ long conserved UTR (3′LCU) is higher than that of the CDS. (**C**) Sequence alignment of the 3′LCUs. (**D-J**) Expression patterns of *mex3b* in *Xenopus* embryos at the four-cell (D,E), early gastrula (F,G), late gastrula (H), early neurula (I) and tailbud (J) stages. (G) Sagittal-hemisection of F. Arrowheads indicate the dorsal blastopore. A, animal view; D, dorsal view; L, lateral view; V, vegetal view.

The 3′LCU promotes translation and destabilization of mRNA

The existence of 3′LCU in the *mex3b* 3′ UTR prompted us to examine the function of this region in the regulation of *mex3b* mRNA. Because the 3′LCU contains several AREs, which are common RNA-destabilizing elements, we first tested whether the 3′LCU promotes mRNA degradation using GFP mRNA reporter constructs (Fig. 2A). Reporter mRNA was injected into the prospective neuroectoderm of *Xenopus* embryos at the four-cell stage and examined at the early neurula stage (stage 13) using WISH. Notably, compared to control mRNAs (GFP, GFP+3′LCUrev and GFP+nc3′UTR), GFP+3′LCU mRNA was markedly degraded (Fig. 2B-E). qRT-PCR confirmed that GFP+3′LCU but not GFP mRNA was significantly decreased between stages 12 (late gastrula) and 13 (Fig. 2H). These data suggest that the 3′LCU has a destabilizing element that responds to some endogenous factors.

To narrow down the region required for the degradative activity, the 3′LCU was divided into four subregions A, B, C and D, based on sequence conservation among vertebrates (see Fig. S1A in the supplementary material). The data showed that subregion A is necessary and sufficient for the degradative activity (Fig. 2F,G), and that this degradation occurs between stage 12 and 13 (see Fig. S2 in the supplementary material). Therefore, we named this element 'late gastrula destabilizing element' (LGDE).

We next examined whether the 3′LCU affects the level of GFP protein. Surprisingly, embryos injected with GFP+3′LCU or GFP+3′LCUrev mRNA showed stronger GFP fluorescence at the neurula stage than those injected with GFP or GFP+nc3′UTR mRNA (Fig. 2I-L). Because both GFP+3′LCU and GFP+3′LCUrev showed translational enhancement, secondary structures of the 3′LCU RNA may be important. Using the 3′LCU deletion constructs, however, we could not assign this translational enhancement activity to a single entity, because all deletion constructs examined had some activity (see Fig. S3 in the supplementary material). Western blot analysis revealed that the increased levels of GFP induced by the 3′LCU were already detectable at the four-cell stage (1.5 hours after mRNA injection) and continued to be observed at later stages (Fig. 2Q). These data suggest that the 3′LCU has elements, named 'translational enhancer elements' (TLEEs), that are distributed in subregions A to D. To examine whether the translational enhancement continued to the neurula stage, we created a destabilized GFP, in which the degradation sequence PEST of ornithine decarboxylase was fused to EGFP. GFP-PEST+3′LCU mRNA-injected embryos exhibited decreased levels of GFP fluorescence at stage 14 (Fig. 2N), consistent with the expectation that GFP-PEST+3′LCU mRNA is degraded at this stage and the GFP-PEST protein is unstable. By contrast, 3′LCUrev still upregulated GFP-PEST protein levels compared with the non-conserved 3′UTR (nc3′UTR) (Fig. 2O,P), suggesting that the TLEEs (actually sequences complementary to TLEEs) also function at the early neurula stage. Taken together, these results suggest that the 3′LCU has at least two types of regulatory elements: LGDE and TLEE.

Mex3b promotes mRNA degradation through the 3′LCU and forms an autoregulatory loop

Because Mex3b has KH domains, we hypothesized that Mex3b could regulate its own mRNA through the 3′LCU. To test this possibility, we examined whether forced expression of Mex3b

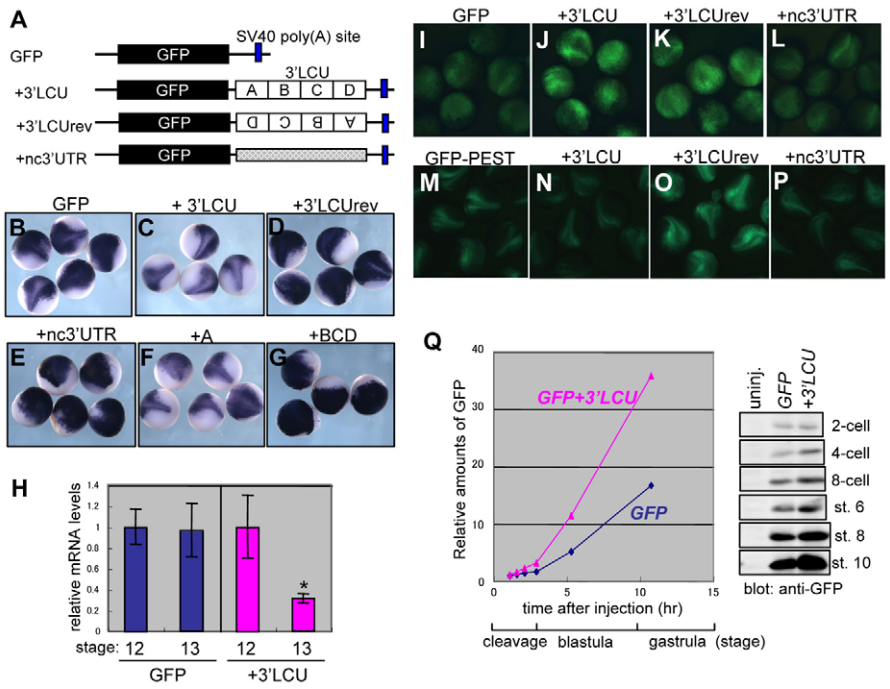

Fig. 2. Reporter mRNA assay for the 3′LCU. (**A**) Schematic representations of GFP mRNA reporter constructs. The GFP or GFP-PEST (not shown) CDS was connected to the 3′LCU, the reverse 3′LCU (3′LCUrev), and a non-conserved region of *mex3b* 3′-UTR (nc3′UTR; positions 1787-2527) as indicated. (**B-H**) Destabilization of reporter mRNA by the 3′LCU and subregion A. The amount of remaining reporter mRNA in injected embryos was examined at stage 13 by WISH using the GFP probe (B-G) or at stages 12 and 13 by qRT-PCR (H). **P*<0.05. (**I-P**) Translational enhancement by the 3′LCU and 3′LCUrev using GFP (I-L) or GFP-PEST (M–P). GFP fluorescence were observed at stage 13 (I-L) or 14 (M-P). (**Q**) Western blot analysis. Reporter mRNA was injected into two dorsal-animal blastomeres at the four-cell stage. All injected embryos were viewed dorsally at the neurula stage. Injected embryos were collected at indicated stages. Amounts of injected reporter mRNA (pg/embryo): 100 (B-P); 500 (Q).

affects the level of reporter mRNA. Although GFP+3′LCU mRNA was degraded to some extent by endogenous factors through the LGDE as shown above, we found that co-injection of *mex3b* mRNA further promoted the degradation of GFP+3′LCU mRNA but not GFP mRNA (Fig. 3A,B). We also showed that this degradation is detectable at stage 9.5 as well as stage 12.5 (see Fig. S4A in the supplementary material), which differs from the LGDE-dependent degradation by endogenous factors after stage 12 (see Fig. S2 in the supplementary material). This indicates that Mex3b destabilizes reporter mRNA in a 3′LCU-dependent manner. By contrast, Mex3b was not able to either promote or reduce the translation of reporter mRNA at stage 7 (see Fig. S4B in the supplementary material) before Mex3b-dependent mRNA degradation occurred, suggesting that Mex3b does not affect the translational enhancement mediated by the TLEEs.

We next assigned a region of the 3′LCU that responds to Mex3b. As shown in Fig. 3C,D, Mex3b destabilized mRNAs, GFP+BCD, +CD and +D, which possess subregion D (panel C; data for +BCD and +CD are not shown), but did not destabilize mRNAs, GFP+ABC, +AB, and +A (panel D; data for +AB and +A are not shown). These data suggest that subregion D is necessary and sufficient for mRNA degradation by Mex3b, and therefore this element was named ‘Mex3b-responsive destabilizing element’ (MRDE). Thus, the 3′LCU has at least two distinct destabilizing elements, LGDE and MRDE, residing in subregions A and D, respectively.

To specify the sequence of MRDE, subregion D was divided into five regions, D1-D5, each of which is about 60 nucleotides long (see Fig. S5A in the supplementary material). Among them, only the D2 construct was destabilized, although weakly, by Mex3b (see Fig. S5B in the supplementary material). Notably, this weak destabilizing activity of D2 was enhanced by adding D1, D3 and D4 but not D5 (see Fig. S5B in the supplementary material). Furthermore, D2 contains a purine-rich stretch followed by a destabilizing sequence AUUUUAUUUUA (see Fig. S5C in the supplementary material), which is similar to the binding site of human MEX3D in the *BCL2* 3′ UTR (Donnini et al., 2004). These data suggest that Mex3b binds to the core sequence of the MRDE in subregion D2 and that the other regions, D1, D3 and D4, are required for full destabilizing activity of the MRDE by binding putative endogenous co-factors of Mex3b.

To examine the physical interaction between Mex3b and the 3′LCU, we next performed RNA immunoprecipitation experiments. Embryos that had been injected with GFP+3′LCU or GFP mRNA as a target and mRNA for HA-tagged protein, were lysed and immunoprecipitated with the anti-HA antibody. Immunoprecipitated protein-RNA complexes were then subjected to RT-PCR for the GFP CDS. As shown in Fig. 3E, GFP+3′LCU mRNA was immunoprecipitated by Mex3b-HA (lane 1). By contrast, smaller amounts of GFP+3′LCU mRNA were brought down by the negative control proteins, ΔKH1+2-4HA and 4HA-globin (lanes 3 and 5), suggesting that Mex3b physically interacts with the 3′LCU through the KH domains. In addition, GFP mRNA was not brought down by Mex3b-4HA (lane 4), indicating that the KH domains of Mex3b specifically bind to the 3′LCU. We conclude from these results that Mex3b has autorepressive activity through the formation of a complex with the 3′LCU, resulting in a negative autoregulatory loop.

The 3′LCU acts as a system for fine-tuning gene expression

We expected that translational enhancement initially predominates over destabilization of mRNA to increase the amount of Mex3b, whereas, when the level of Mex3b becomes high enough to destabilize *mex3b* mRNA, the rate of production of Mex3b is reduced. This combined regulation provides a buffering action, which leads to fine-tuning gene expression. To test this hypothesis, we designed the experiment that mimics the endogenous state, using pCS DNA expression constructs that have the CMV promoter and the CDS for tagged Mex3b with or without the 3′LCU or subregion D (Fig. 4A,D). Expression levels of Mex3b were varied by injecting different amounts of DNA expression constructs, and the amounts of transcript and protein were analyzed at stage 12.5/13. In both cases of the 3′LCU and subregion D, increased amounts of DNA expression constructs led to increased levels of mRNA (Fig. 4B,E)

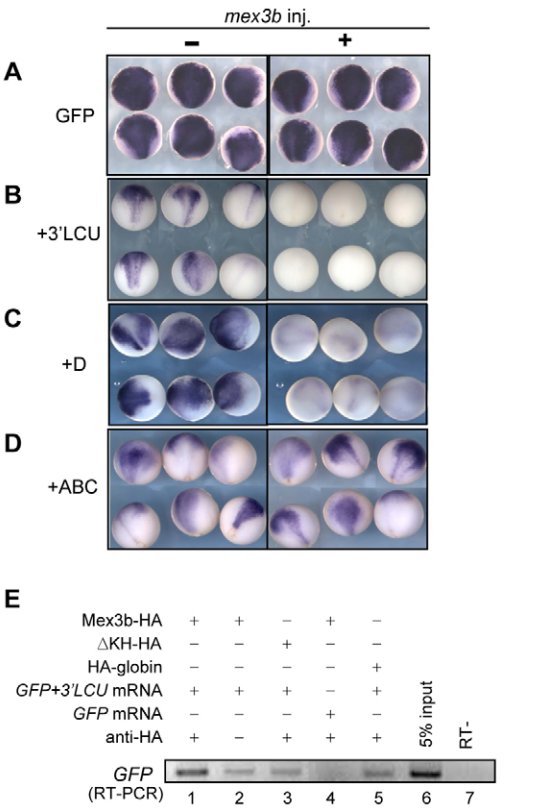

Fig. 3. Destabilization of reporter mRNA by Mex3b through the 3′LCU. (**A-D**) Destabilization by Mex3b through the 3′LCU and subregion D. Injection and WISH were performed as described in Fig. 2. *mex3b* mRNA (63 pg/embryo) was co-injected with reporter mRNA (right panels). (**E**) Co-immunoprecipitation of GFP+3′LCU mRNA with Mex3b. GFP+3′LCU or GFP reporter mRNA (100 pg) was co-injected with mRNA for *mex3b*-HA, *ΔKH1+2*-HA or HA-*globin* (1 ng). Reporter mRNA was co-immunoprecipitated with the anti-HA antibody and analyzed by RT-PCR.

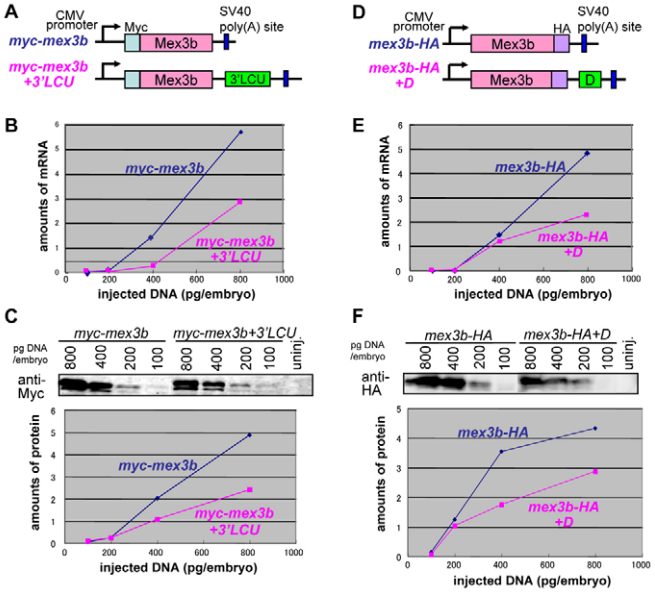

Fig. 4. A negative autoregulatory loop of Mex3b. (**A-C**) *myc-mex3b* and the 3′LCU. (**D-F**) *mex3b-HA* and subregion D. Schematic representations of expression constructs are shown (A,D). Myc-Mex3b and Mex3b-HA exhibited basically the same activity. Embryos injected with each DNA construct were lysed at stage 13. Transcripts were quantitated by qRT-PCR using the SV40 primer set (B,E). Proteins were quantitated by immunoblotting with the anti-Myc (C) or anti-HA (F) antibody. The abscissa, amounts of injected DNA (pg/embryo); the ordinate, relative expression (arbitrary units).

and protein (Fig. 4C,F), but both levels were much less with the 3′LCU or subregion D than the control. These data suggest that the negative autoregulatory loop operates through the MRDE in the 3′LCU and subregion D. Timecourse experiments also confirmed that the accumulation of Mex3b protein is delayed by subregion D (see Fig. S6 in the supplementary material). We noticed that an injection of 100 pg of CMV-*myc-mex3b*+3′LCU slightly upregulated the Mex3b protein level compared with the control (compare the protein bands of the western blot in Fig. 4C), supporting the translational enhancement activity of the 3′LCU. Taken together, these data suggest that the translational enhancement and the negative autoregulatory loop through the 3′LCU form a fine-tuning system to maintain an appropriate level of Mex3b protein by their buffering action.

Effects of overexpression and knockdown of Mex3b on its own mRNA and on early embryogenesis

We next asked whether this negative autoregulatory loop through the 3′LCU operates in vivo and what the role of Mex3b is in early *Xenopus* embryogenesis. To address these questions, we first overexpressed Mex3b in the dorsal mesoderm or dorsal ectoderm region by injecting mRNA into the dorsal equatorial region or the dorsal animal pole region, respectively, at the four-cell stage (Takada et al., 2005). Overexpression of Mex3b in the dorsal mesoderm resulted in the loss of *Xbra* expression at the early gastrula stage (Fig. 5A), but it did not affect the expression of *gsc* and *Xlim1* (see Fig. S7A,B in the supplementary material). Because *Xbra* expression is known to be induced by both FGF and activin/Nodal signaling (Smith et al., 1991), whereas *gsc* and *Xlim1* are induced by activin/Nodal but not by FGF signaling (Cho et al., 1991; Taira et al., 1992), the data suggest that Mex3b specifically inhibits FGF signaling. Overexpression of Mex3b in the neuroectoderm reduced endogenous *mex3b* expression (Fig. 5B), which is in good agreement with its autorepression activity. Mex3b also decreased, although not strongly, the expression of the anterior marker *otx2* (Fig. 5C) and the posterior marker genes *cdx4/Xcad3* and *hoxd1* (Fig. 5D,E) at the neurula stage, but did not affect a pan-neural marker, *sox2* (Fig. 5F), a neural crest marker, *msx1*, and an anterior mesoderm marker, *crescent* (data not shown). Notably, forced expression of Myc-ΔKH1+2, which lacks KH domains, increased the level of the endogenous *mex3b* mRNA (Fig. 5G), suggesting that Myc-ΔKH1+2 functions as a dominant-negative mutant. At tailbud stages, overexpression of Mex3b in the dorsal mesoderm and neuroectoderm both exhibited a short axis phenotype (Fig. 5H-J). These data suggest that Mex3b is involved in AP patterning of the neural plate and in mesoderm formation.

To analyze the requirement for Mex3b during early embryogenesis, we next performed loss-of-function experiments using antisense morpholino oligos (MOs). We designed two MOs, *mex3b*MO1 and *mex3b*MO2, which targeted different sites of the *mex3b* 5′ UTR, and a five-base mismatched MO (5mmMO) as a control. We first examined the specificity of *mex3b*MO1 and

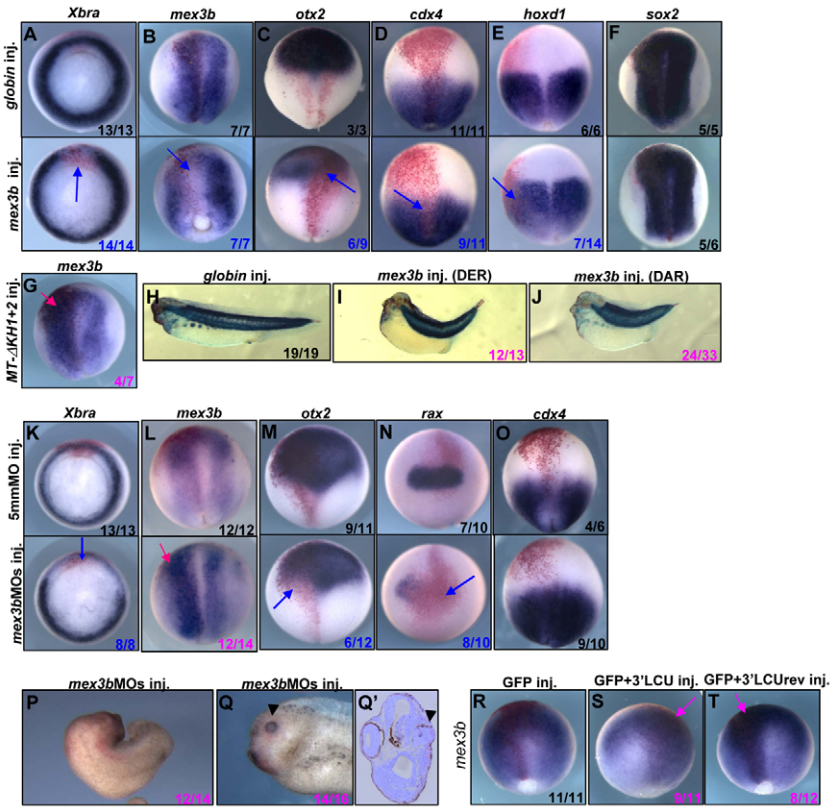

Fig. 5. Functional analysis of Mex3b in early embryogenesis. (**A-J**) Overexpression of *mex3b* by mRNA injection. (**K-Q′**) Knockdown of *mex3b* by MO injection. mRNA (1 ng) or MO (50 ng) was co-injected with nβ-gal mRNA as a tracer into one blastomere in the dorsal equatorial region (A,I,K,P; indicated by DER) or the neuroectoderm (the rest). nβ-gal staining (red) indicates the injected side. Arrows in blue or magenta indicate reduced or increased expression, respectively. Frequency of specimen with the indicated phenotype is shown in the right bottom of each panel in blue (reduction), magenta (enhancement) or black (no change). Embryos were injected with *globin* (upper panels of A-F,H), *mex3b* (lower panels of A-F,I,J) or Myc-ΔKH1+2 (G) mRNA as indicated, and were subjected to WISH for genes as indicated at stage 10.5 (A) or stage 13 (B-G), or to immunostaining of somites with the 12/101 antibody followed by clearing with benzyl benzoate/benzyl alcohol (H-J). 5mmMO- or *mex3b*MO-injected embryos were subjected to WISH at stage 10.5 (K) and stage 13 (L-O), or observed for morphological appearances at stage 35 (P,Q). Transverse section (Q′) of Q indicates small eye (arrowheads in Q,Q′) (**R-T**) Effects of the 3′LCU on *mex3b* expression. Embryos were injected with GFP, GFP+3′LCU or GFP+3′LCUrev mRNA (3 ng/embryo), and subjected to WISH for endogenous *mex3b* mRNA at stage 12.5. Arrows in S and T indicate increased expression.

showed that it specifically inhibited the protein synthesis from 5′ UTR-*mex3b* mRNA (see Fig. S7D in the supplementary material). Because both *mex3b*MO1 and *mex3b*MO2 gave similar phenotypes, we used a mixture of them (referred to as *mex3b*MOs) for subsequent experiments.

Injection of *mex3b*MOs in the dorsal equatorial region markedly decreased the expression of *Xbra* (Fig. 5K) but not of *chordin*, *gsc* and *Xlim1* (see Fig. S7J-L in the supplementary material) and caused severe open-yolk-plug phenotypes at the tailbud stages (Fig. 5P). This result is somewhat unexpected, because overexpression of Mex3b also inhibits *Xbra* expression (Fig. 5A; and see Discussion). However, the effect of *mex3b*MOs on *Xbra* expression is specific, because rescue experiments showed that the inhibition of *Xbra* expression by the MOs was recovered by co-injection with *mex3b* mRNA (see Fig. S7E-I in the supplementary material).

Importantly, injection of *mex3b*MOs into the prospective neuroectoderm region increased the endogenous expression of *mex3b*, strongly suggesting that Mex3b destabilizes its own mRNA in vivo. We also found that *mex3b*MOs decreased the expression of anterior markers, *otx2* and *rax* (Fig. 5M,N) possibly by increasing posteriorizing signals. However, *mex3b*MOs did not expand *cdx4* expression in an anterior direction (Fig. 5O), leading to the possibility that the anterior boundary of *cdx4* is determined by negative regulation, which could not be overcome by increasing posteriorizing signals. In fact, we have observed that FGF20, which has the ability to inhibit *otx2* expression (see Fig. S7M in the supplementary material), was not able to expand *cdx4* expression in the dorsal region (see Fig. S7N in the supplementary material; indicated by black arrow), but expanded it in the lateral region (see Fig. S7N in the supplementary material; indicated by magenta arrow), implying that *cdx4* is positively regulated by FGF signaling but negatively regulated for the anterior boundary by other signaling pathways. At the tailbud stage, small eye phenotypes were observed (Fig. 5Q,Q′), consistent with *otx2* and *rax* reduction at the neurula stage. Together with the results of the gain-of-function experiments, these data suggest that Mex3b is required for AP patterning in the neural plate and mesodermal differentiation in the marginal zone, and that the negative autoregulatory loop of Mex3b is operating in vivo.

We hypothesized that the negative autoregulation of *mex3b* mRNA occurs through the 3′LCU in vivo. If this is the case, excess amounts of 3′LCU should deplete possible 3′LCU-binding proteins (3′LCU-BPs), including Mex3b, from the cell, and excess amounts of the complementary strand of the 3′LCU (3′LCUrev) should hybridize to the 3′LCU of *mex3b* mRNA to prevent 3′LCU-BPs from binding. To test this possibility, we injected a large amount of GFP+3′LCU or GFP+3′LCUrev mRNA into embryos and showed that both injected mRNAs increased the amount of endogenous *mex3b* mRNA (Fig. 5R–T). These data indicate that the level of *mex3b* mRNA in vivo is negatively regulated through the 3′LCU.

Mex3b affects the FGF responsiveness of the cell

The phenotypes caused by overexpression and knockdown of Mex3b suggest the possible relationship between Mex3b and FGF signaling, because *cdx4* and *Xbra* are direct targets of FGF signaling (Haremaki et al., 2003; Northrop and Kimelman, 1994; Pownall et al., 1996; Smith et al., 1991). To examine whether Mex3b inhibits FGF signaling, we first performed animal cap assays. As shown in Fig. 6A, Mex3b inhibited *Xbra* expression induced by FGF2, similar to a dominant-negative FGFR1, XFD. In control experiments, Mex3b did not inhibit *gsc* expression induced by activin (Fig. 6B), suggesting that Mex3b specifically inhibits FGF signaling. To further address this, we performed reporter analysis using *cdx4-luc*,

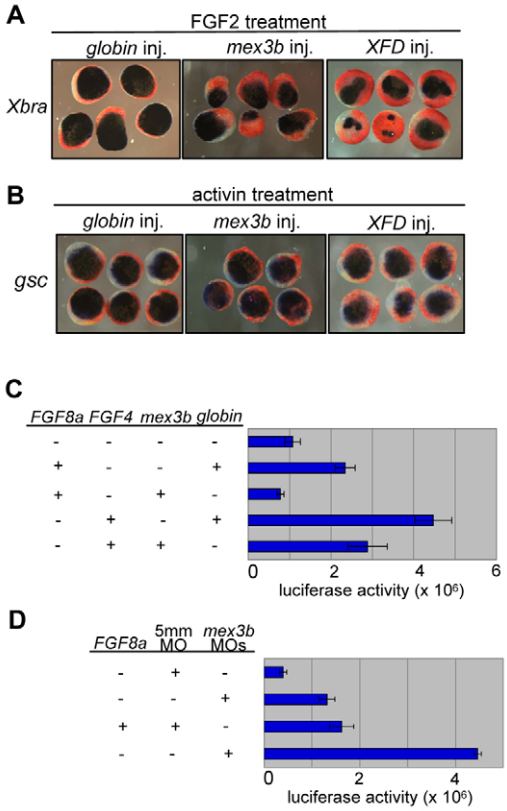

Fig. 6. Inhibition of FGF signaling by Mex3b. (**A**,**B**) Animal cap assay. Animal caps were dissected from embryos injected with globin or mex3b or XFD mRNA (1 ng/embryo) and treated with FGF2 (100 ng/ml) or activin (20 ng/ml). *Xbra* or *gsc* expression was examined by WISH at stage 10.5 equivalent. (**C**,**D**) FGF reporter assay. Reporter DNA *cdx4/Xcad3-luc* (100 pg) with or without *fgf8* mRNA (100 pg) or *fgf4* DNA (10 pg) was co-injected with *mex3b* mRNA (1 ng; C) or *mex3b*MOs (50 ng; D), and injected embryos were assayed for luciferase activity at stage 12.5/13. Bars represent the mean±s.e.m.

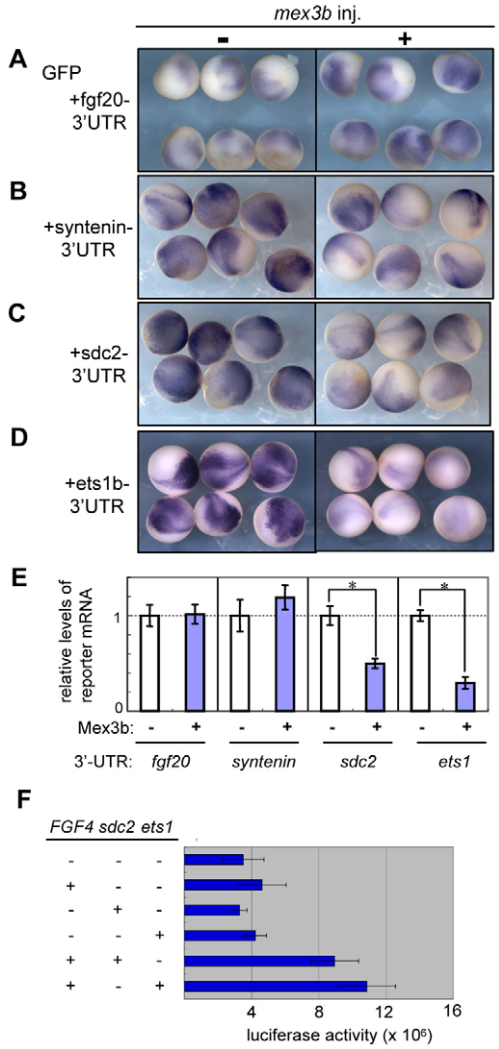

Fig. 7. Analysis of *sdc2* and *ets1b* for Mex3b targets and FGF signaling. (**A-E**) Response of the 3′ UTRs of *sdc2* and *ets1b* to Mex3b-mediated destabilization. Injection, WISH (A-D) and qRT-PCR (E) were performed as described in Fig. 2. GFP reporter mRNA containing the 3′ UTR of indicated genes (100 pg/embryo) was co-injected with (right panel) or without (left panel) *mex3b* mRNA (63 pg). Reporter mRNA remaining in the embryos were examined at stage 12.5/13. Note that the 3′ UTR of *fgf20* (A), *syntenin* (B), *sdc2* (C) or *ets1* (D) destabilized reporter mRNA to some extent in respond to endogenous factors (left panels), but only the 3′ UTR of *sdc2* (C) or *ets1* (D) responded to Mex3b for mRNA destabilization (right panels). (**F**) FGF reporter assay. Reporter DNA *cdx4/Xcad3-luc* (100 pg) was co-injected with *fgf4* DNA (10 pg), *sdc2* mRNA (100 pg) and *ets1* (100 pg) as indicated, and injected embryos were assayed for luciferase activity at stage 12.5/13.

in which the luciferase gene is driven by the *cdx4* promoter and intron 1 containing FGF response elements; this reporter is upregulated in the dorsal ectoderm in an FGF-dependent manner or activated by FGF signaling in dissociated animal cap cells (Haremaki et al., 2003). As shown in Fig. 6C, expression of *fgf8* or *fgf4* upregulated luciferase activity of *cdx4-luc* in the ventral ectodermal region, and this activity was inhibited by co-injection of *mex3b* mRNA (Fig. 6C). Conversely, *mex3b*MOs further upregulated luciferase activity induced by FGF8 (Fig. 6D). Because expression of *cdx4-luc* is reportedly affected by Tcf3 or β-catenin (Haremaki et al., 2003), we asked whether Mex3b modulates canonical Wnt signaling. TOPFLASH reporter analysis showed that Mex3b did not inhibit activation of the reporter gene by Wnt8 (data not shown), suggesting that Mex3b or *mex3b*MOs affect *cdx4-luc* through modulation of FGF signaling. These data suggest that higher or lower levels of Mex3b determine lower or higher sensitivity, respectively, of recipient cells to FGF.

To analyze where Mex3b acts in FGF signaling, *cdx4-luc* was activated in different ways. Luciferase activity induced by constitutively active (ca)-FGFR1 or ca-Ras was decreased by Mex3b, suggesting that Mex3b acts downstream of Ras (see Fig. S8A in the supplementary material). We next examined whether Mex3b inhibits ERK phosphorylation by FGF4 using animal cap assays but it did not do so (see Fig. S8B in the supplementary material), suggesting that Mex3b mainly affects a FGF signal transducer(s) downstream of, or parallel with, ERK, or both.

Microarray screening of Mex3b target mRNAs

The data so far suggest that Mex3b regulates FGF signaling by destabilizing some mRNAs in a similar manner to autorepression. To identify such putative target mRNAs of Mex3b, we performed differential screening using *Xenopus* oligo DNA microarray. Target mRNAs, if any, would be expected to be regulated in a

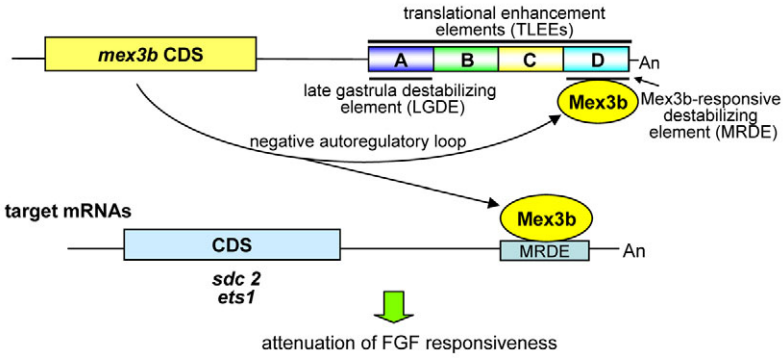

Fig. 8. A model for post-transcriptional regulation by Mex3b. Mex3b protein levels are determined by fine-tuning mechanisms involving TLEEs and the LGDE, and a negative autoregulatory loop through the MRDE. Mex3b in turn controls the stability of target mRNAs such as *ets1b* and *sdc2*, which may contribute to regulate FGF responsiveness. An, poly(A) tail.

fashion similar to that of *mex3b* mRNA and to be decreased in Mex3b-overexpressed embryos and increased in *mex3b*MOs-injected embryos. Based on this expectation, we carried out two sets of differential screening with (1) wild-type Mex3b versus Myc-ΔKH1+2 and (2) 5mmMO versus *mex3b*MOs. mRNA or MO was injected into the prospective neuroectoderm region of embryos with GFP mRNA as a tracer, and the embryos in which GFP fluorescence was detected in the neural plate were collected at the early neurula stage. To maximize the difference in the levels of affected mRNAs, the neural plate was isolated from these embryos. Total RNA was extracted from these neuroectoderm pieces and verified by semi-quantitative RT-PCR for *mex3b* mRNA.

To select possible Mex3b target mRNAs, we used criteria of a 1.5-fold difference in set 1 (wt-Mex3b/Myc versus ΔKH1+2) and a 1.2-fold difference in set 2 (5mmMO versus *mex3b*MOs) so that selected genes include *mex3b*, which is considered as an internal positive control in this microarray experiment. We assigned *Xenopus* and/or mouse RefSeq ID(s) for 6826 genes from the 28,310 tags in total. These genes were divided into three groups according to the following conditions: group 1, candidates of Mex3b target genes (ΔKH1+2/Mex3b ratio of more than 1.5 or a *mex3b*MOs/5mmMO ratio of more than 1.2; 221 genes; see the footnote of Table S1 in the supplementary material); group 2, negative controls, the genes with expression that would not be regulated by Mex3b (ΔKH1+2/Mex3b ratio of less than 1.1 and a *mex3b*MOs/5mmMO ratio of less than 1.1; 155 genes); and group 3, the remaining 6447 genes. We performed GOstat analysis (Beissbarth and Speed, 2004), which categorizes genes based on gene ontology (GO) terms. However, we could not find any specific GO terms concentrated in the group 1 genes, and thereby could not expect any common functions of Mex3b targets from microarray analysis (see the footnote of Table S2 in the supplementary material). These data imply that Mex3b directly or indirectly regulates various mRNAs, which are involved in diverged cellular functions.

sdc2 and *ets1* as Mex3b target mRNAs

Because functional analyses suggest the involvement of Mex3b in FGF signaling, we used the microarray data to seek possible FGF-signaling components. We picked *fgf20*, *ets1* and *syntenin* (syndecan-binding protein) from the 221 possible targets (in both set 1 and set 2), and *sdc2* from set 1 (752 tags). We first focused on *fgf20*. However, although *fgf20* mRNA was downregulated by forced expression of Mex3b in the whole embryo (see Fig. S7C in the supplementary material), mRNA reporter analysis showed that the 3′ UTR of *fgf20* did not respond to Mex3b for destabilization (Fig. 7A). Therefore, we directly analyzed 3′ UTRs of *sdc2*, *ets1b* and *syntenin*. We found that Mex3b specifically destabilizes the 3′ UTRs of *sdc2* and *ets1b* but not of *syntenin* mRNAs (Fig. 7B-D). qRT-PCR analysis confirmed the above results (Fig. 7E). Because *sdc2* and *ets1b* are reportedly expressed in the neural plate and the posterior region at the gastrula stage, respectively (Meyer et al., 1997; Teel and Yost, 1996), their expression domains overlap with that of *mex3b*, supporting the idea that *sdc2* and *ets1b* mRNAs can be regulated by Mex3b.

Using the *cdx4-luc* reporter construct, we showed that Sdc2 or Ets1 enhances luciferase activity induced by FGF4 (Fig. 7F). Furthermore, co-expression of Sdc2 and Ets1 upregulated the reporter gene, which was further enhanced by FGF4 (see Fig. S8C in the supplementary material). These data suggest that Sdc2 and Ets1 are signal transduction components of FGF, and that *sdc2* and *ets1b* mRNAs are likely to be direct targets of Mex3b and therefore at least partly involved in the attenuation of FGF responsiveness by Mex3b.

DISCUSSION

In this study, we have analyzed the function of the RNA-binding protein Mex3b and its 3′UTR regulatory region, the 3′LCU, in early *Xenopus* embryogenesis. Based on our data, we propose the following model of post-transcriptional regulation of *mex3b* mRNA (Fig. 8). The 3′LCU has at least three distinct elements. The first type is the translational enhancer element (TLEE), distributed in four subregions A to D; the second type is the late gastrula destabilizing element (LGDE) in subregion A; and the third type is the Mex3b-responsive destabilizing element (MRDE) in subregion D. Of these elements, the negative autoregulatory loop through the MRDE is a key component in the maintenance of the level of Mex3b protein. The TLEEs also contribute to the maintenance of the protein level by rapid upward regulation of *mex3b* mRNA translation when the protein level is decreased. The LGDE affects the mRNA level through some as yet unidentified trans-acting factors, which act at the late gastrula stage and perhaps later. Thus, these three distinct elements constitute a fine-tuning system for *mex3b* mRNA that determines and maintains an appropriate level of Mex3b by providing a buffering action against fluctuations. Mex3b at a certain level in turn controls the half-life of target mRNAs including *sdc2* and *ets1b*, which are probably involved in FGF responsiveness. This model provides a new mechanism for fine-tuning the control of mRNAs as well as a novel role of post-translational regulation in determining the level of cellular responsiveness to signaling molecules.

Several types of post-transcriptional autoregulation by RNA-binding proteins have been reported. For example, *Drosophila* ELAV binds to its own 3′UTR, as does the mouse homolog Mel-N1, and this binding increases the stability of mRNA by competing with other factors that destabilize the mRNA (Abe et al., 1996; Borgeson

and Samson, 2005; Samson, 1998). TTP destabilizes its own mRNA as well as other mRNAs through binding to AUUUA sequences (Brooks et al., 2004). The poly(A) binding protein PABP downregulates its own translation or decreases the amount of its own mRNA in a cell-type-specific manner (Hornstein et al., 1999). Among them, the Mex3b autoregulation mechanism is similar to that of TTP. However, Mex3b has a characteristic 3′UTR, 3′LCU, that possesses translational enhancer elements in addition to autoregulatory elements.

Derepression mechanisms for translational enhancement are well known. The best example of a derepression mechanism is that of the cytoplasmic polyadenylation element (CPE) during oocyte maturation. Before maturation, the CPE-binding protein (CPEB) inhibits translation by binding to the CPE, whereas, when maturation begins, translation is initiated by derepression of CPEB activity upon its phosphorylation by Aurora kinase (Kuersten and Goodwin, 2003). By contrast, the 3′LCU of *mex3b* enhances translation, possibly by the binding of trans-acting factors to the secondary structures of the 3′LCU. Recently, it has been reported that the 3′ UTR of *nanos2* enhances its translation, as distinct from derepression (Tsuda et al., 2006), but the mechanism of enhancement is unknown. More recently, it has been revealed that microRNAs upregulate the translation of TNFα mRNA through recruiting Argonaute and FXR1 (Vasudevan et al., 2007). In all cases, further studies are necessary to clarify the mechanisms of translational enhancement through the 3′ UTR. Thus, our data provide a novel 3′-regulatory module that is composed of elements for both positive regulation and negative autoregulation. Furthermore, we have shown that this regulatory module is actually operating in developing embryos.

We have shown that Mex3b can destabilize mRNAs for *sdc2* and *ets1* and inhibits FGF signaling. To date, various negative and positive regulators of FGF signaling have been reported, including the negative regulators Sprouty, Sef and Mkp3 (Furthauer et al., 2002; Hacohen et al., 1998; Kawakami et al., 2003) and the positive regulator xHtrA1 (Hou et al., 2007), which stimulates long-range FGF signaling by cleaving proteoglycans. All of these are induced by FGF and regulate the range of FGF signaling through protein modification of FGF signal components, providing the feedback regulation of FGF signaling. Another type of regulator for FGF signaling is p53, which inhibits the translation of *fgf2* mRNA by preventing the formation of 80S ribosome through its binding to the 5′ UTR of *fgf2* mRNA (Galy et al., 2001a; Galy et al., 2001b). However, to our knowledge, post-transcriptional regulation of FGF signaling components has not been reported. Thus, our data provide the first evidence of the regulation of FGF responsiveness through mRNA degradation by RNA-binding proteins.

What is the role of Mex3b in FGF signal transduction? In AP patterning of the neuroectoderm, FGF signals act as morphogens to regionalize the neuroectoderm along the AP axis in a concentration-dependent manner (Dubrulle and Pourquie, 2004; Kengaku and Okamoto, 1995). In this context, Mex3b is required to control the levels of key FGF components at the mRNA level to fine-tune the level of FGF signaling. The effects of such fine-tuning mechanisms at post-transcriptional levels may be relatively subtle compared with transcriptional regulation, but they are absolutely necessary for normal development, as we have shown in this study using overexpression and knockdown of Mex3b. In the mesoderm, overexpression of Mex3b decreases *Xbra* expression, which is consistent with the requirement of FGF signaling for Xbra expression. However, knockdown of Mex3b also decreases Xbra expression. We do not have sufficient data to explain this result, but one possibility is that Mex3b morpholino downregulates Xbra expression through upregulation of some unidentified Mex3b targets, which directly or indirectly inhibits *Xbra* expression.

Our data indicate that subregion D of the 3′LCU is necessary and sufficient for the negative autoregulation of Mex3b. Interestingly, only subregion D is conserved among human *MEX3B*, *MEX3C*, *MEX3D* and *Xenopus mex3c*, suggesting that the autoregulation is a common mechanism of Mex3 family members. Supporting this idea, we found that Mex3b can destabilize GFP reporter mRNA containing subregion D of *Xenopus mex3c* (see Fig. S5 in the supplementary material). We also found that the amphioxus *mex3* gene has the 3′LCU-like sequence (see Fig. S1 in the supplementary material). Therefore, the entire 3′LCU was probably acquired in the ancestral *mex3* gene before two rounds of whole genome duplication occurred during vertebrate evolution, and subregions A-C have been changed or lost in *mex3* family members other than *mex3b*. In invertebrates, *C. elegans mex-3* does not have the 3′LCU. Mex-3 is anteriorly localized in *C. elegans* embryos and inhibits the posterior fate. Thus, even if the protein level of Mex-3 is in excess in the anterior region, it does not affect the posterior formation, implying that *C. elegans* Mex-3 does not require the fine-tuning mechanisms through the 3′LCU. By contrast, *Xenopus* Mex3b is expressed in the entire neuroectoderm and is likely to be involved in maintaining an appropriate level of FGF signaling. In this situation, for AP patterning to be precisely determined, an appropriate level of Mex3b protein is necessary. It should be noted that in *C. elegans* Mex-3 downregulates mRNA of *caudal*, possibly by directly binding to its 3′ UTR, whereas in *Xenopus* Mex3b indirectly downregulates *Cdx4/Xcad3*, probably through inhibiting FGF signaling. Thus, our data suggest the interesting possibility that the existence of the 3′LCU enables Mex3b to regulate the AP patterning of neural tissue through the fine-tuning of FGF responsiveness.

To date, it has been shown that human MEX3D (TINO) destabilizes the mRNA for BCL2, which inhibits apoptosis, and that MEX3C is putatively involved in ‘essential hypertension’. Because subregion D is conserved in *MEX3C* and *MEX3D* mRNAs, our data concerning *mex3b* autoregulation may be applicable to the understanding of molecular mechanisms of other developmental processes and human diseases in which *mex3* genes are involved.

Acknowledgements

We thank D. Turner, R. Rupp and J Lee for pCS2+, pCS2+MT and pCS2+nβ-gal, E. De Robertis for *gsc*; Y. Sasai for *sox2* and *chd*; H. Okamoto for the *Xcad3* luciferase reporter construct; H. Ide for *fgf8*; M. Pannese for pGEM3-Xotx2; K. Yokoyama for pXFGF-20 and pSP36-XFGF-20; J. Smith for Xbra, M. Jamrich for Rx2a, H. Sive for hoxd1, and M. Hagiwara and T. Nojima for discussion. This work was supported in part by a Grant-in-Aid for Science Research from the Ministry of Education, Science, Sports, and Culture of Japan (M.T.); by research fellowship of the Japan Society for the Promotion of Science (H.T.); and by the Global COE Program (Integrative Life Science Based on the Study of Biosignaling Mechanisms), MEXT, Japan (H.T. and H.M.).

Supplementary material

Supplementary material for this article is available at
http://dev.biologists.org/cgi/content/full/136/14/2413/DC1

References

Abe, R., Yamamoto, K. and Sakamoto, H. (1996). Target specificity of neuronal RNA-binding protein, Mel-N1: direct binding to the 3′ untranslated region of its own mRNA. *Nucleic Acids Res.* **24**, 2011-2016.

Barreau, C., Paillard, L. and Osborne, H. B. (2005). AU-rich elements and associated factors: are there unifying principles? *Nucleic Acids Res.* **33**, 7138-7150.

Beissbarth, T. and Speed, T. P. (2004). GOstat: find statistically overrepresented Gene Ontologies within a group of genes. *Bioinformatics* **20**, 1464-1465.
Borgeson, C. D. and Samson, M. L. (2005). Shared RNA-binding sites for interacting members of the Drosophila ELAV family of neuronal proteins. *Nucleic Acids Res.* **33**, 6372-6383.
Brooks, S. A., Connolly, J. E. and Rigby, W. F. (2004). The role of mRNA turnover in the regulation of tristetraprolin expression: evidence for an extracellular signal-regulated kinase-specific, AU-rich element-dependent, autoregulatory pathway. *J. Immunol.* **172**, 7263-7271.
Buchet-Poyau, K., Courchet, J., Le Hir, H., Seraphin, B., Scoazec, J. Y., Duret, L., Domon-Dell, C., Freund, J. N. and Billaud, M. (2007). Identification and characterization of human Mex-3 proteins, a novel family of evolutionarily conserved RNA-binding proteins differentially localized to processing bodies. *Nucleic Acids Res.* **35**, 1289-1300.
Chen, C. Y. and Shyu, A. B. (1995). AU-rich elements: characterization and importance in mRNA degradation. *Trends Biochem. Sci.* **20**, 465-470.
Cho, K. W., Blumberg, B., Steinbeisser, H. and De Robertis, E. M. (1991). Molecular nature of Spemann's organizer: the role of the Xenopus homeobox gene goosecoid. *Cell* **67**, 1111-1120.
Donnini, M., Lapucci, A., Papucci, L., Witort, E., Jacquier, A., Brewer, G., Nicolin, A., Capaccioli, S. and Schiavone, N. (2004). Identification of TINO: a new evolutionarily conserved BCL-2 AU-rich element RNA-binding protein. *J. Biol. Chem.* **279**, 20154-20166.
Draper, B. W., Mello, C. C., Bowerman, B., Hardin, J. and Priess, J. R. (1996). MEX-3 is a KH domain protein that regulates blastomere identity in early C. elegans embryos. *Cell* **87**, 205-216.
Dubrulle, J. and Pourquie, O. (2004). fgf8 mRNA decay establishes a gradient that couples axial elongation to patterning in the vertebrate embryo. *Nature* **427**, 419-422.
Furthauer, M., Lin, W., Ang, S. L., Thisse, B. and Thisse, C. (2002). Sef is a feedback-induced antagonist of Ras/MAPK-mediated FGF signalling. *Nat. Cell Biol.* **4**, 170-174.
Galy, B., Creancier, L., Prado-Lourenco, L., Prats, A. C. and Prats, H. (2001a). p53 directs conformational change and translation initiation blockade of human fibroblast growth factor 2 mRNA. *Oncogene* **20**, 4613-4620.
Galy, B., Creancier, L., Zanibellato, C., Prats, A. C. and Prats, H. (2001b). Tumour suppressor p53 inhibits human fibroblast growth factor 2 expression by a post-transcriptional mechanism. *Oncogene* **20**, 1669-1677.
Guzman, B., Cormand, B., Ribases, M., Gonzalez-Nunez, D., Botey, A. and Poch, E. (2006). Implication of chromosome 18 in hypertension by sibling pair and association analyses: putative involvement of the RKHD2 gene. *Hypertension* **48**, 883-891.
Hacohen, N., Kramer, S., Sutherland, D., Hiromi, Y. and Krasnow, M. A. (1998). sprouty encodes a novel antagonist of FGF signaling that patterns apical branching of the Drosophila airways. *Cell* **92**, 253-263.
Haremaki, T., Tanaka, Y., Hongo, I., Yuge, M. and Okamoto, H. (2003). Integration of multiple signal transducing pathways on Fgf response elements of the Xenopus caudal homologue Xcad3. *Development* **130**, 4907-4917.
Hornstein, E., Harel, H., Levy, G. and Meyuhas, O. (1999). Overexpression of poly(A)-binding protein down-regulates the translation or the abundance of its own mRNA. *FEBS Lett.* **457**, 209-213.
Hou, S., Maccarana, M., Min, T. H., Strate, I. and Pera, E. M. (2007). The secreted serine protease xHtrA1 stimulates long-range FGF signaling in the early Xenopus embryo. *Dev. Cell* **13**, 226-241.
Huang, N. N., Mootz, D. E., Walhout, A. J., Vidal, M. and Hunter, C. P. (2002). MEX-3 interacting proteins link cell polarity to asymmetric gene expression in Caenorhabditis elegans. *Development* **129**, 747-759.
Kawakami, Y., Rodriguez-Leon, J., Koth, C. M., Buscher, D., Itoh, T., Raya, A., Ng, J. K., Esteban, C. R., Takahashi, S., Henrique, D. et al. (2003). MKP3 mediates the cellular response to FGF8 signalling in the vertebrate limb. *Nat. Cell Biol.* **5**, 513-519.
Kengaku, M. and Okamoto, H. (1995). bFGF as a possible morphogen for the anteroposterior axis of the central nervous system in Xenopus. *Development* **121**, 3121-3130.
Kuersten, S. and Goodwin, E. B. (2003). The power of the 3′ UTR: translational control and development. *Nat. Rev. Genet.* **4**, 626-637.
Liu, K. J. and Harland, R. M. (2005). Inhibition of neurogenesis by SRp38, a neuroD-regulated RNA-binding protein. *Development* **132**, 1511-1523.
Meyer, D., Durliat, M., Senan, F., Wolff, M., Andre, M., Hourdry, J. and Remy, P. (1997). Ets-1 and Ets-2 proto-oncogenes exhibit differential and restricted expression patterns during Xenopus laevis oogenesis and embryogenesis. *Int. J. Dev. Biol.* **41**, 607-620.
Minakhina, S. and Steward, R. (2005). Axes formation and RNA localization. *Curr. Opin. Genet. Dev.* **15**, 416-421.
Nieuwkoop, P. D. and Faber, J. (1967). *Normal Table of Xenopus laevis (Daudin)*. Amsterdam: North Holland.
Northrop, J. L. and Kimelman, D. (1994). Dorsal-ventral differences in Xcad-3 expression in response to FGF-mediated induction in Xenopus. *Dev. Biol.* **161**, 490-503.
Perrone-Bizzozero, N. and Bolognani, F. (2002). Role of HuD and other RNA-binding proteins in neural development and plasticity. *J. Neurosci. Res.* **68**, 121-126.
Pownall, M. E., Tucker, A. S., Slack, J. M. and Isaacs, H. V. (1996). eFGF, Xcad3 and Hox genes form a molecular pathway that establishes the anteroposterior axis in Xenopus. *Development* **122**, 3881-3892.
Samson, M. L. (1998). Evidence for 3′ untranslated region-dependent autoregulation of the Drosophila gene encoding the neuronal nuclear RNA-binding protein ELAV. *Genetics* **150**, 723-733.
Satou, Y. (1999). posterior end mark 3 (pem-3), an ascidian maternally expressed gene with localized mRNA encodes a protein with Caenorhabditis elegans MEX-3-like KH domains. *Dev. Biol.* **212**, 337-350.
Sevignani, C., Calin, G. A., Siracusa, L. D. and Croce, C. M. (2006). Mammalian microRNAs: a small world for fine-tuning gene expression. *Mamm. Genome* **17**, 189-202.
Shinga, J., Itoh, M., Shiokawa, K., Taira, S. and Taira, M. (2001). Early patterning of the prospective midbrain-hindbrain boundary by the HES-related gene XHR1 in Xenopus embryos. *Mech. Dev.* **109**, 225-239.
Smith, J. C., Price, B. M., Green, J. B., Weigel, D. and Herrmann, B. G. (1991). Expression of a Xenopus homolog of Brachyury (T) is an immediate-early response to mesoderm induction. *Cell* **67**, 79-87.
Suga, A., Hikasa, H. and Taira, M. (2006). Xenopus ADAMTS1 negatively modulates FGF signaling independent of its metalloprotease activity. *Dev. Biol.* **295**, 26-39.
Taira, M., Jamrich, M., Good, P. J. and Dawid, I. B. (1992). The LIM domain-containing homeo box gene Xlim-1 is expressed specifically in the organizer region of Xenopus gastrula embryos. *Genes Dev.* **6**, 356-366.
Takada, H., Hattori, D., Kitayama, A., Ueno, N. and Taira, M. (2005). Identification of target genes for the Xenopus Hes-related protein XHR1, a prepattern factor specifying the midbrain-hindbrain boundary. *Dev. Biol.* **283**, 253-267.
Takahashi, N., Tochimoto, N., Ohmori, S. Y., Mamada, H., Itoh, M., Inamori, M., Shinga, J., Osada, S. and Taira, M. (2005). Systematic screening for genes specifically expressed in the anterior neuroectoderm during early Xenopus development. *Int. J. Dev. Biol.* **49**, 939-951.
Teel, A. L. and Yost, H. J. (1996). Embryonic expression patterns of Xenopus syndecans. *Mech. Dev.* **59**, 115-127.
Tsuda, M., Kiso, M. and Saga, Y. (2006). Implication of nanos2-3′UTR in the expression and function of nanos2. *Mech. Dev.* **123**, 440-449.
van de Wetering, M., Cavallo, R., Dooijes, D., van Beest, M., van Es, J., Loureiro, J., Ypma, A., Hursh, D., Jones, T., Bejsovec, A. et al. (1997). Armadillo coactivates transcription driven by the product of the Drosophila segment polarity gene dTCF. *Cell* **88**, 789-799.
Vasudevan, S., Tong, Y. and Steitz, J. A. (2007). Switching from repression to activation: microRNAs can up-regulate translation. *Science* **318**, 1931-1934.
Yamamoto, S., Hikasa, H., Ono, H. and Taira, M. (2003). Molecular link in the sequential induction of the Spemann organizer: direct activation of the *cerberus* gene by Xlim-1, Xotx2, Mix.1, and Siamois, immediately downstream from Nodal and Wnt signaling. *Dev. Biol.* **257**, 190-204.